Electron diffraction and high-resolution transmission electron microscopy of the high temperature crystal structures of GexSb2Te3+x (x=1,2,3) phase change material

Kooi, Bart; De Hosson, J.T.M.

Published in:
Journal of Applied Physics

DOI:
10.1063/1.1502915

Publication date:
2002

Electron diffraction and high-resolution transmission electron microscopy of the high temperature crystal structures of $Ge_xSb_2Te_{3+x}$ ($x=1,2,3$) phase change material

B. J. Kooi and J. Th. M. De Hosson[a)]
Department of Applied Physics, Materials Science Centre and Netherlands Institute for Metals Research, University of Groningen, Nijenborgh 4, 9747 AG Groningen, The Netherlands

(Received 14 March 2002; accepted for publication 2 July 2002)

The crystal structures of $GeSb_2Te_4$, $Ge_2Sb_2Te_5$, and $Ge_3Sb_2Te_6$ were determined using electron diffraction and high-resolution transmission electron microscopy. The structure determined for the former two crystals deviates from the ones proposed in the literature. These crystal structures were developed jointly upon cooling of liquid $Ge_2Sb_2Te_5$. A stacking disorder parallel to the basal plane was observed that increases with increasing cooling rates. For the $Ge_xSb_2Te_{3+x}$ ($x=1,2,3$) crystals it is shown that an a,b,c stacking holds with an alternating stacking of x GeTe double layers identically present in binary GeTe and one Te–Sb–Te–Te–Sb– repeat unit also present in binary Sb_2Te_3. A stacking disorder is a logical consequence of building crystals with these two principal units. On the other hand, it is likely that all stable crystals of the Ge–Sb–Te systems are an ordered sequence of these two units. Some of the implications of these findings of the stable and metastable crystal structures that develop from amorphous $Ge_2Sb_2Te_5$ are presented so as to understand the crucial crystallization process in $Ge_2Sb_2Te_5$ phase change material. © *2002 American Institute of Physics.* [DOI: 10.1063/1.1502915]

I. INTRODUCTION

In recent years thin films composed of $Ge_2Sb_2Te_5$ have received increasing scientific attention because of their current use in optical recording as rewriteable memory media.[1–9] Amorphous spots in a crystalline surrounding act as bits of information. Both continuous laser light and short laser pulses at various higher power densities can be employed to read, write, and/or erase those local amorphous areas and thus the phase changes in the material are exploited. The attractiveness of $Ge_2Sb_2Te_5$ originates from its clear optical contrast and its excellent reversibility between the amorphous and crystalline state, its high thermal stability at room temperature, and the high crystallization rates.[8] Particularly, this latter feature is becoming increasingly important because of increasing demands on the rates of data transfer. Crystallization is considered the rate-limiting process, because amorphization is inherently a much faster process.[5,6] It has been argued that a possible disadvantage of the use of $Ge_2Sb_2Te_5$ is that the crystalline state used in phase change optical recording applications is metastable,[10,11] whereupon after an increased heat input (to higher temperatures) a stable structure develops. On the other hand, the demanded high crystallization rate of $Ge_2Sb_2Te_5$ is possibly a direct consequence of the metastability of the phase, which allows for a much easier crystallization process due to fewer constraints on the short range diffusion and ordering of the different atomic species. A precise knowledge of the structures of the metastable and stable crystalline phases is considered to be of importance in arriving at a complete understanding of the driving forces for crystallization. Recently, several papers have dealt with the structure of the metastable phase.[7,8] In contrast, on the high temperature stable crystal structure of $Ge_2Sb_2Te_5$ only a single relatively older report exists.[12] The purpose of the present work is to verify the correctness of the proposed stable crystal structure. Furthermore, rapid cooling rates have been used to solidify bulk $Ge_2Sb_2Te_5$ from the melt in order to obtain insight into how the structure responds to this phase transition starting from an amorphous phase. This is in contrast to the amorphous–crystalline transition at low temperatures that is exploited in phase change optical recording.

II. CRYSTAL STRUCTURES

Stable binary crystal structures in the Ge–Sb–Te system involve the phase GeTe (with a low and high temperature modification, both show a composition range with a width of about 1 at. %) and the rather stoichiometric phase Sb_2Te_3.[13] Ge and Sb turn out to be immiscible in the solid state.[13] GeTe at low temperature ($<400\,^{\circ}C$) has a trigonal (R-$3m$) structure with a (rhombohedral) lattice constant of 0.5996 nm and $\alpha=88.18°$.[14,15] At higher temperature it transforms to the NaCl ($B1$) type structure with a lattice constant of 0.60 nm (and most importantly α changes to 90°). Sb_2Te_3 possesses also a trigonal R-$3m$ (tetradymite) structure with $a=1.0426$ nm and $\alpha=23°31'$.[16] Using hexagonal axes GeTe has $a'=0.417$ and $c'=1.071$ nm with an a,b,c stacking sequence of close packed planes along the c'-axis of Te–Ge–Te–Ge–Te–Ge– (i.e., the close packed planes consist of the atoms of only one element). The high temperature GeTe structure can also be considered in this way, but then a' is 0.424 nm. In Sb_2Te_3 the lattice parameters are $a'=0.425$ and $c'=3.04$ nm with an a,b,c stacking along the c'-axis Te–

a)Electronic mail: hossonj@phys.rug.nl

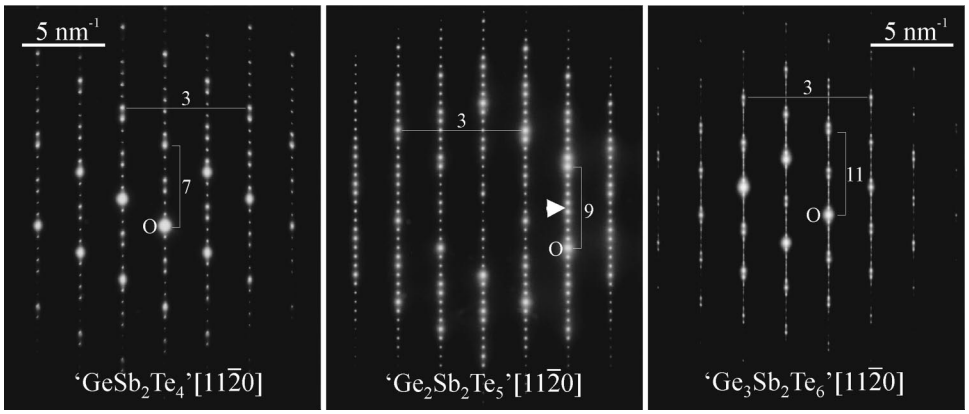

FIG. 1. SAED patterns from three different crystals in the same $Ge_2Sb_2Te_5$ alloy cooled moderately fast from the melt. The crystals from left to right correspond to trigonal structures with as hexagonal axes $a'=0.425$ nm and $c'=4.10$, $c'=1.827$, and $c'=6.26$ nm, respectively, which could be ascribed to $GeSb_2Te_4$, $Ge_2Sb_2Te_5$, and $Ge_3Sb_2Te_6$, respectively. In all cases viewing is along [11-20].

Sb–Te–Te–Sb– (three times repeated, because the a,b,c stacking requires that the number of planes along the c'-axis within the unit cell is always a multiple of 3).

This rather extensive information is intriguing when considering the metastable and stable crystalline structures of $Ge_2Sb_2Te_5$. If we consider the stable structure, taking the immiscibility of Ge and Sb into account, and noting that the a' lattice constants of GeTe and Sb_2Te_3 are fairly similar, then for $Ge_2Sb_2Te_5$ the structure becomes just an alternation in c'-direction of a four layer block of GeTe and one repeat-unit of Sb_2Te_3; that is, a stacking according to Te–Ge–Te–Sb–Te–Te–Sb–Te–Ge– and a trigonal cell with hexagonal axes with dimensions $a'\approx 0.42$, $c'\approx 1.72$ nm. Here, the cell is now primitive because the number of layers is nine, which is directly a multiple of three. Indeed, for $Ge_2Sb_2Te_5$ it is reported that $a'=0.420$ and $c'=1.696$ nm and the space group is primitive rhombohedral (P-3m1).[12] However, the stacking sequence was derived as Te–Sb–Te–Ge–Te–Te–Ge–Te–Sb–; that is, the Ge and Sb positions are exchanged with the two Ge layers instead of the Sb separated by the Te double layer, not in accordance with the structures of GeTe and Sb_2Te_3. In a recent paper lattice constants $a'=0.422$ and $c'=1.718$ nm have been reported without any further structural analysis.[3]

The metastable crystalline phase of $Ge_2Sb_2Te_5$ turns out to have the NaCl-type structure, with the Te atoms on one fcc sublattice (e.g., Cl sites) and with the Ge and Sb atoms and (thus) 20% of vacancies distributed randomly over the other fcc sublattice.[7,8] The lattice constant, depending on the exact composition and temperature, is $a=0.60$ nm.[7,8] This structure is thus almost identical to the one of binary GeTe. In this sense it is remarkable that Ge and Sb want to occupy the same close-packed plane. The repulsion between Ge and Sb can be counteracted by the neighboring Te planes, and possibly the vacancies are essential for stabilizing the structure. Nonetheless it is not remarkable that this structure is metastable.

Based on the GeTe and Sb_2Te_3 (and Ge–Sb) binary structures it may be expected that, in general, the phases $Ge_xSb_2Te_{3+x}$ (with x an integer) consist of an alternation in c'-direction of one repeat unit of Sb_2Te_3 and a block consisting of $2x$ layers GeTe. The purpose of this article is to show that this picture holds and that the stacking sequences proposed in Ref. 17 for $GeSb_2Te_4$ and in Ref. 12 for $Ge_2Sb_2Te_5$ are erroneous. Furthermore, the structure of $Ge_3Sb_2Te_6$ will be assessed using electron diffraction and high-resolution transmission electron microscopy (HRTEM). The structure proposed in Ref. 12 for $GeSb_4Te_7$ is in agreement with the present picture, because the unit cell in the c'-direction consists of two repeat units of Sb_2Te_3 separated by a 2 layer GeTe block.

Perfect crystals are not likely in practice and stacking disorder is likely to occur in the Ge–Sb–Te system. For instance, $Ge_2Sb_2Te_5$ crystals may show local $GeSb_2Te_4$ stacking that has to be compensated by the local presence of $Ge_3Sb_2Te_6$. Far from equilibrium, many possible stacking sequences with GeTe double layers and Sb_2Te_3 repeat units may be possible as long as the overall composition is finally attained.

III. EXPERIMENTAL PROCEDURES

$Ge_2Sb_2Te_5$ alloys were produced by mixing the pure components (Ge:6 N, Sb and Te both 5 N) in an evacuated quartz tube at 750 °C. The melt was solidified using three different cooling rates: (i) furnace cooled, (ii) pulled out of the furnace on a metal plate at room temperature, and (iii) quenching the liquid material into water (dispersing the melt into small solid pieces). Pieces of the alloy according to (i) and (ii) were also annealed 24 h at 400 °C. TEM samples were prepared by grinding, dimpling, and ion milling (using a Gatan PIPS at 4 kV with Ar sputtering from $\pm 6°$) 3 mm discs to electron transparency. Small pieces of the water-quenched sample were ground to a fine powder in a mortar and dispersed in isopropanol. A droplet of the suspension was put on a Si-nitride membrane and dried before insertion in the TEM. The selected area electron diffraction patterns and HRTEM images were obtained using a JEOL 4000 EX/II operating at 400 kV and energy dispersive x-ray spectra were recorded using a JEOL 2010F operating at 200 kV equipped with an EDAX detector containing a so-called ''super-ultra'' thin window.

IV. RESULTS

Selected-area electron diffraction (SAED) patterns originating from three different grains in the same TEM sample of $Ge_2Sb_2Te_5$ that was cooled relatively fast from the melt are presented in Fig. 1. Here, the quartz tube was pulled out

of the furnace on a metal plate at room temperature. Analysis of the central pattern indicates a *d*-spacing corresponding to the row of finely spaced reflections of 1.727 nm and orthogonal to this a *e*-spacing of 0.368 nm. Because no pattern with more densely spaced reflections in these two orthogonal directions could be found, the 1.727 and 0.368 nm values correspond to the lowest index reflections possible. On the basis of the intensity modulation of the reflections, that is, a period of 9 along the row with finely spaced reflections and a period of 3 perpendicular to that, and because no systematic absences were found (along the line with a multiple of 3, reflections are present on each finely spaced row), a primitive trigonal unit cell with $a'=0.425$ and $c'=1.727$ nm with nine layers according to the a,b,c stacking along the c'-axis is found to hold for the crystal. These results agree with the ones obtained in Ref. 12 for $Ge_2Sb_2Te_5$, but the lattice constants found match better with the more recent data ($a'=0.422$ and $c'=1.718$ nm).[3] The SAED patterns on the left and on the right in Fig. 1 yields $a'=0.425$, $c'=1.367$ nm and $a'=0.425$, $c'=2.087$ nm, respectively. Thus, the a' value is identical for all three grains and only the c' values vary. The period of the intensity modulation along the c'-axis is 7 for the left image and 11 for the right image. So, instead of a crystal with a 9-layer repeat unit along the c'-axis, crystals with 7 and 11 layer repeat units are present. The a,b,c stacking implies that the number of planes along the c'-axis in the unit cell is a multiple of 3. The repeat units of 7 or 9 layers do not satisfy this requirement, and hence the unit cell will have a real c'-axis that is a multiple of 3 larger, i.e., $c'=4.10$ nm for the left pattern and $c'=6.26$ nm for the right one. This multiple of 3 longer c'-axis could also have been derived directly from the systematic absences in the patterns. In contrast to the central pattern now along the line with a multiple of 3, reflections are not present on each finely spaced row, but only repeat after each third row. Starting from the 9-layer structure of $Ge_2Sb_2Te_5$ the repeat unit in the grain of the left pattern contains two layers less and of the right two layers more. In principle this could be either a Ge–Te or a Sb–Te double layer. Deriving the thickness of these double layers from the known trigonal (R-3m) GeTe and Sb_2Te_3 crystal structures yields 0.357 and approximately 0.38 nm, respectively. According to the SAED patterns the experimentally determined thickness is 0.360, and this matches much better with a Ge–Te double layer than with a Sb–Te one. Thus, the grain of the left pattern is likely to be $GeSb_2Te_4$ and of the right pattern $Ge_3Sb_2Te_6$.

Streaking can be observed along the c'-axis in principle in all three SAED patterns and denotes an amount of disorder in the stacking sequence of the planes along the c'-axis. However, streaking is clearly most pronounced for $Ge_3Sb_2Te_6$, rather weak for $GeSb_2Te_4$ and almost absent for $Ge_2Sb_2Te_5$. Possibly this variation in the extent of streaking is a measure for the thermodynamic stability of the three different crystal structures under the conditions given. Because the overall composition of the alloy is $Ge_2Sb_2Te_5$ it is not remarkable that this crystal shows the least stacking disorder. $Ge_3Sb_2Te_6$ may be unstable but as long as $GeSb_2Te_4$ is present it cannot disappear due to the constraint of the overall composition.

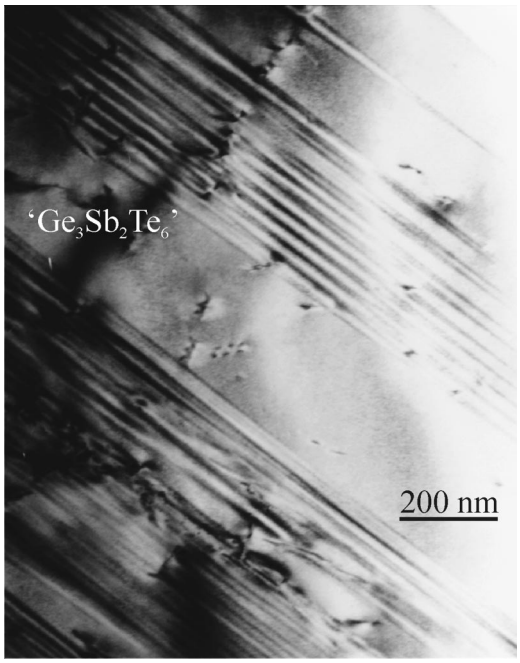

FIG. 2. Conventional TEM image of typical stacking fault contrast in a $Ge_3Sb_2Te_6$ crystal, showing the relative high amount of stacking disorder parallel to the basal planes in the structure.

The degree of stacking disorder can easily be observed in conventional TEM images. Figure 2 presents an example for a $Ge_3Sb_2Te_6$ grain in which the typical stacking fault contrast can be observed from inclined basal planes in the TEM foil. Still, a lamella with a thickness of about 300 nm is present in which no stacking faults occur. Also some dislocation contrast can be recognized in Fig. 2.

As a matter of course, it is questionable whether the analysis of crystal structures for relatively quickly cooled samples yields the crystal structure of stable crystals. However, after annealing a slowly furnace cooled alloy 24 h at 400 °C, identical diffraction patterns were observed. Trying to quench the melt more rapidly by breaking a quartz tube with the molten alloy in water (dispersing the alloy into small solid pieces) also showed the same crystal structures present. The fraction of stacking defects, that is, the amount of streaking, varies as a consequence of these different conditions, but the basic underlying structures remain intact.

In Ref. 12 the proposed stacking sequence for $Ge_2Sb_2Te_5$ along the c'-axis is Te–Sb–Te–Ge–Te–Te–Ge–Te–Sb–. Knowing the GeTe and Sb_2Te_3 crystal structures this sequence is an anomaly and a more logical structure is Te–Ge–Te–Sb–Te–Te–Sb–Te–Ge–, that is, Ge and Sb exchange positions. Simulation of the diffraction patterns for these two sequences, using full dynamical diffraction (MacTempas[18]), were carried out, keeping all other parameters fixed, for example, convergence angle 0.2 mrad and crystal thickness 7 nm. The resulting patterns are shown in Fig. 3; the top one is based on the anomalous sequence of Ref. 12 (''Old'') and the bottom one is the sequence proposed here (''New''). The intensity of the reflections is deliberately low in order to make the variations in intensity more distinct. For this reason some reflections may disap-

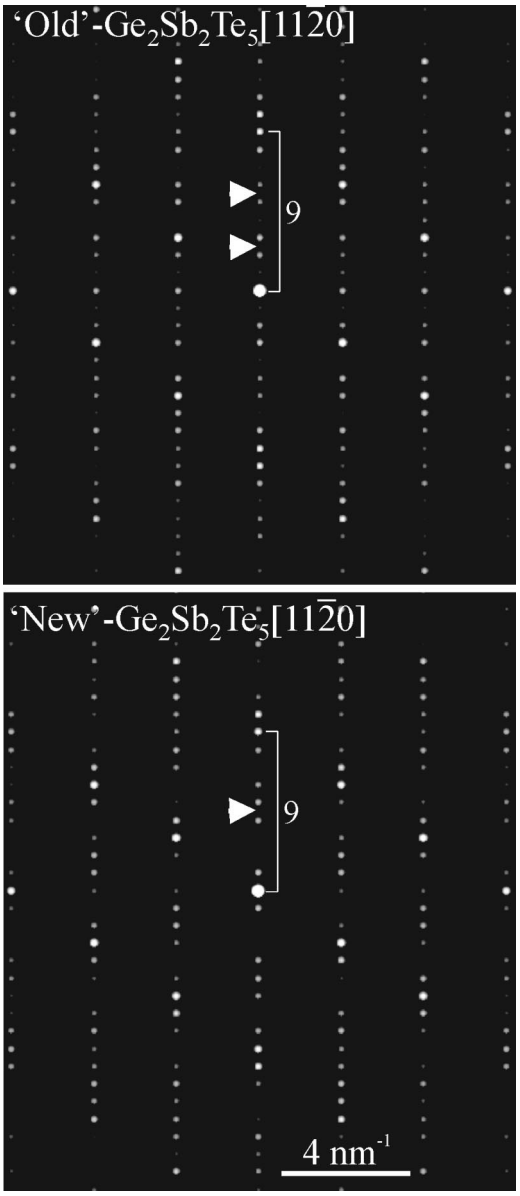

FIG. 3. Simulated electron diffraction patterns for $Ge_2Sb_2Te_5$ viewed along [11-20] based on dynamical diffraction. The top pattern shows the results for a Te–Sb–Te–Ge–Te–Te–Ge–Te–Sb– stacking sequence along the c'-axis proposed in Ref. 12 and the bottom one for a sequence where the Ge and Sb basal planes are interchanged. Comparison of these simulated patterns with the experimental one in the center of Fig. 1 shows unambiguously that the bottom pattern is better matching.

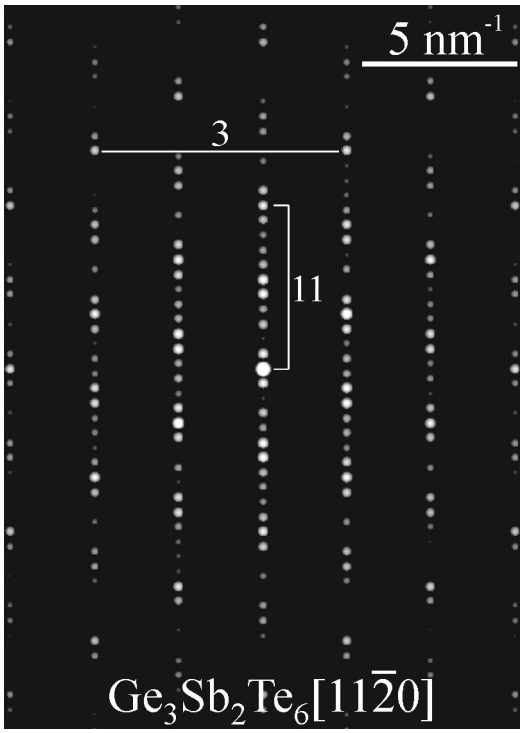

FIG. 4. Simulated electron diffraction pattern for $Ge_3Sb_2Te_6$ viewed along [11-20] based on dynamical diffraction. Comparison of this simulated pattern with the experimental one on the right in Fig. 1 shows a good agreement.

pear, but are in fact not really absent. A comparison between the two simulated patterns in Fig. 3 with the central pattern in Fig. 1 makes clear that the new sequence matches the experimental results better than the old one. It should be realized that there is no need to perform an elaborate fitting procedure. Of course, both satisfy the intensity modulation with a period of 9 along the c'-axis and a period of 3 along the a'-axis. However, one of the clear differences is that the sub- period intensity modulation in the period of 9, with one additional maximum for the 0004 and 0005 reflection indicated by an arrow in the central pattern of Fig. 1 is reproduced well in the bottom pattern of Fig. 1 and not in the top pattern, where two additional maxima occur.

So far, no previous reports on the crystal structure of $Ge_3Sb_2Te_6$ have been found. Figure 4 presents a simulation of its diffraction pattern for the [11-20] zone axis (lattice constants $a'=0.425$ nm, $c'=6.252$ nm, space group $R\text{-}3m$ with the a,b,c stacking sequence proposed above, convergence angle of 0.2 mrad, crystal thickness 10 nm). Of course, apart from streaking, this simulated diffraction pattern reproduces excellently the experimental one on the right in Fig. 1.

In order to verify the stacking sequence, atomic scale HRTEM images were recorded. In Fig. 5 a HRTEM image of a ''$Ge_3Sb_2Te_6$'' crystal is presented with a simulated image as inset (middle left). The simulation parameters were: 400 kV, C_s: 1 mm, convergence angle:1 mrad, spread in defocus: 10 nm, defocus: -10 nm, thickness: 6 nm. Because Sb and Te are heavy elements that are neighbors in the periodic table; their scattering factors are almost identical and therefore dark or bright spots on the position of the atomic columns of Sb or Te are also nearly identical. Thus, deviating contrast in the layered structure stems from the close packed Ge planes. This simple reasoning is confirmed by the image simulations performed for different defocus values of the microscope and different thicknesses of the samples. Ideas for a direct structure reconstruction, that is, solving the inverse problem[19,20] are based on the channeling effect, where the electrons of the incoming wave remain highly localized on the atomic columns, and the exit wave thus directly represents the projected structure, also reflecting the chemical content of the columns. In the HRTEM image in Fig. 5 it can be seen that each time a block of small dots (Sb and Te atoms) are separated by three rows containing elongated

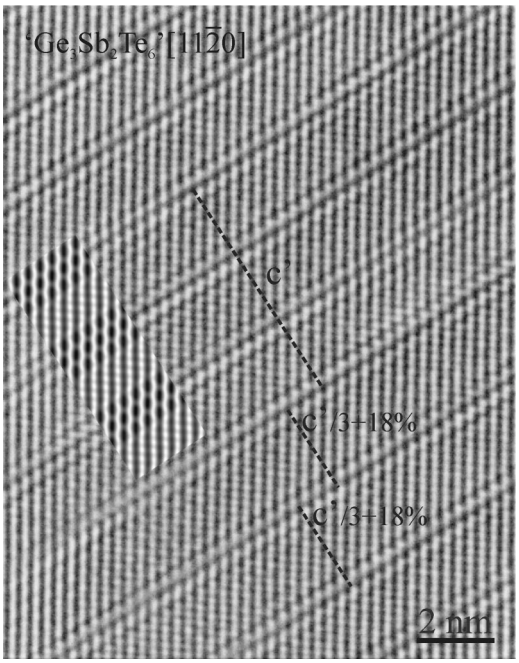

FIG. 5. HRTEM image of $Ge_3Sb_2Te_6$ viewed along [11-20] with a simulated image as inset. The more than 6 nm length of the c'-axis of the hexagonal unit cell is indicated by the white dashed line denoted as c′ also illustrating the a,b,c stacking of the structure. The presence of stacking disorder is shown by the two neighboring repeat units that are 18% longer than the other ones of $Ge_3Sb_2Te_6$. The additional thickness of the repeat unit originates from an additional Sb–Te double layer.

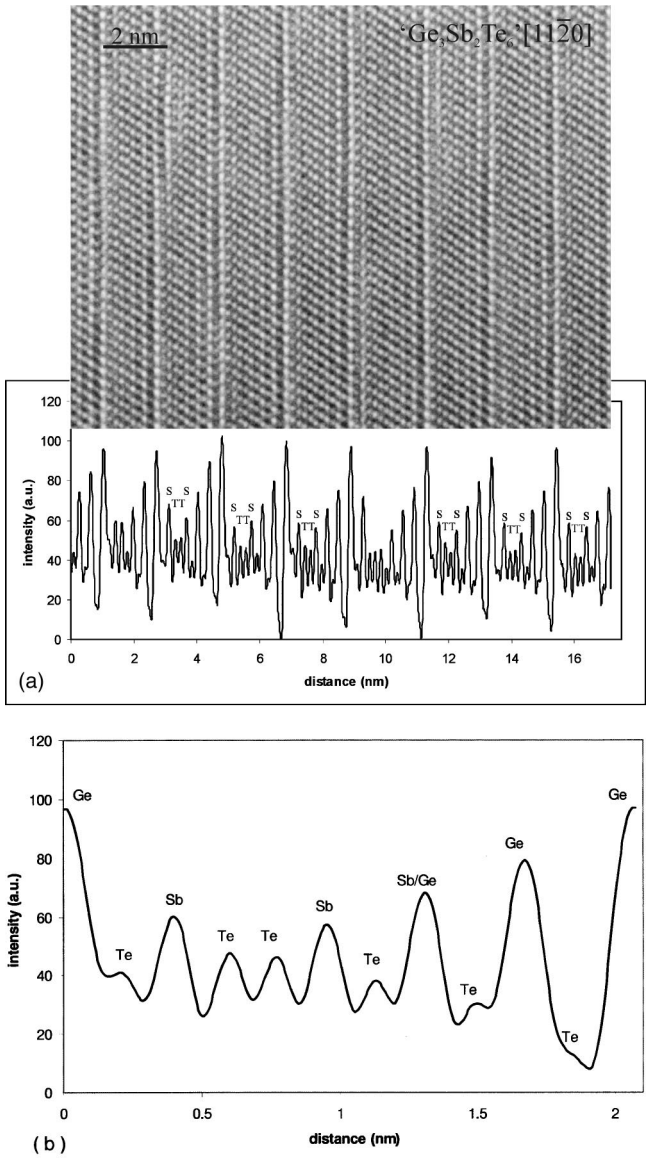

FIG. 6. (a) HRTEM image of $Ge_3Sb_2Te_6$ viewed along [11-20] with a line profile at the bottom obtained by integrating the intensity in the HRTEM image parallel to the edge-on basal planes in the projected structure. The intensities of the maximum in the line profile appears to directly reflect the chemical nature of the corresponding basal plane in the HRTEM image. (b) The average of five repeat units present in the line profile of (a) with the chemical interpretation of the maximum in intensities that reproduces the expected structure of the repeat unit in $Ge_3Sb_2Te_6$.

black dots. These three rows with deviating intensity correspond to the three Ge–Te double layers present in the $Ge_3Sb_2Te_6$ structure. Hence, on an atomic level the structure proposed on the basis of electron diffraction is also confirmed. The length of the c'-axis of somewhat more than 6 nm can also be derived on the basis of the HRTEM image as is indicated by the dashed line in the center of the image; if we start at say an a position, then after what seems one repeat unit we are on a c position, after two repeat units on a b position, and only after the third unit we are back at the a position.

Stacking disorder can be observed in Fig. 5 because all repeat units along the c'-axis have the same thickness corresponding to the 11 layers of $Ge_3Sb_2Te_6$, but the two neighboring blocks have a thickness that is about 18% to 19% larger than the repeat unit ($c'/3$) of $Ge_3Sb_2Te_6$ (as indicated in Fig. 5). Therefore, the additional thickness is about 0.38 nm, which agrees well with the thickness of the Sb–Te– double layer (see above). In addition, the contrast in the HRTEM image associated with the additional thickness agrees with the one that would originate from the Sb_2Te_3 block.

Figure 6(a) presents another HRTEM image of this ''$Ge_3Sb_2Te_6$'' crystal with a different defocus and a different thickness than in Fig. 5. In the image the bright dots are on the atomic columns. Because we know that each atomic plane having its normal parallel to the c'-axis contains in principle only the atoms of a single element, it is logical to average the intensities in the image along the atomic planes and to transform the image into a line profile. The resulting line profile is also shown in Fig. 6(a). We may try to match the maximum in intensities to the atomic species. Because it is clear from the image simulations that the largest deviations in intensity originate from the Ge planes, we can more or less judge their positions, that is, peaks with highest maximum. In between these regions with the bright Ge peaks in the line profile, two neighboring peaks with the same lowest intensity are present. Because we know that in between the Ge–Te double layers an Sb_2Te_3 block with a central Te–Te double layer is present, these neighboring peaks with the same low intensity can be ascribed to this Te–Te double layer. On both sides of this double layer Sb should be present, and apparently the Sb gives peaks with slightly higher intensity than Te, but clearly lower than Ge. These central blocks of Sb–Te–Te–Sb– when clearly observable

are indicated in the line profile by "$^{S}_{TT}{}^{S}$". The line profile thus seems to clearly reflect the different chemical species in the individual layers. The average of five periods in the line profile, which appear identical in Fig. 6(a), is presented in Fig. 6(b), showing the basic repeat unit in the $Ge_3Sb_2Te_6$ structure with the chemical interpretation of each maximum indicated. Clearly, the expected structure for the repeat unit in $Ge_3Sb_2Te_6$ is reproduced. One plane having intermediate intensity between the ones ascribed to pure Ge and Sb planes is denoted as a plane containing both Ge and Sb atoms. In view of the known metastable NaCl-type structure of $Ge_2Sb_2Te_5$, where Te occupies the Cl sites and Ge and Sb and 20% vacancies mix randomly on the Na sites, it may not be surprising that what in the above results are consistently called pure Ge or Sb planes may in fact be impurified with atoms of the other element. However, because this will make the discussion more complicated and because it is very hard to supply direct evidence for the presence of Sb on the Ge planes and vice versa, this mixing effect can not receive serious attention in this article. In addition, errors will be made when intensities in the line profile are directly linked to the chemical composition. This procedure and the results are only within certain precautions correct for (the phase image of) the exit wave if the distance between the atomic columns is not too small[19,20] and are not correct for an image where the transfer function of the microscope comes into play. For instance, residual beam tilt (always present to some extent in the image because a voltage center and not a comma-free alignment is performed) will lead for instance to differences in intensity for the "*a*" and "*b*" stacked planes in simple close-packed hexagonal structures even if the chemical composition of both plane types is identical.[21] Thus, the intensities in the line profile of Fig. 6 are a complicated interplay of structural and imaging parameters and can in principle not be interpreted intuitively. For instance, the different intensities of what are interpreted as the Ge planes in the line-profile Fig. 6(b) can be largely influenced by beam tilt. Nevertheless, although the interpretation in Fig. 6(b) with the denoted chemical elements is tentative, it remains nicely in accordance with the expectation for $Ge_3Sb_2Te_6$.

V. DISCUSSION

Quenching liquid $Ge_2Sb_2Te_5$ in water did not result in a solid amorphous structure. The metastable phase of $Ge_2Sb_2Te_5$, that is, the NaCl-type structure with Te occupying one fcc sublatticed (e.g., the Cl sites) and Ge and Sb and 20% vacancies randomly mixed on the other sublattice (Na sites), was also not observed. However, clear deviations from the stable $Ge_2Sb_2Te_5$ structure, that is, trigonal with a primitive hexagonal cell with Te–Ge–Te–Sb–Te–Te–Sb–Te–Ge– stacking along the c'-axis, do occur upon quenching. Two other dominating structures corresponding to stochiometrics of $GeSb_2Te_4$ and $Ge_3Sb_2Te_6$ were also observed. It is clear that nuclei of these three different phases form in the same melt and can grow simultaneously. Within each crystal, disorder in stacking sequences is present. Higher cooling rates probably imply a larger fraction of $GeSb_2Te_4$ and $Ge_3Sb_2Te_6$ crystals and certainly imply more faults in stacking order. Basic units in all the crystals, including those with a large fraction of disorder, are Ge–Te double layers, also present in binary GeTe, and Te–Sb–Te–Te–Sb– and Sb–Te double layers, also present in binary Sb_2Te_3. It may be that all possible stable crystal structures in the ternary Ge–Sb–Te system will be built out of these basic units and will have a,b,c stacking. A decrease of stability will first increase the stacking disorder and will subsequently increase the amount of intermixing of the atoms in the Sb and Ge planes. Finally, a metastable phase with a,b,c stacking develops that is now known as the crystalline phase that is exploited in $Ge_2Sb_2Te_5$ phase change material.

Despite the strong resemblance between the structures of the melt and the solid amorphous phase employed in phase change optical recording, the characteristics of crystallization from the melt versus an amorphous solid are largely different. Dominant differences are the larger amount of latent heat released during the transition from liquid to solid, and the much faster diffusion during crystallization from the melt than from the solid amorphous phase. Diffusion rates are different not only due to the difference in temperature, but also because of diffusion in the melt versus the solid state. Therefore, formation of the metastable phase from the melt is less likely to occur.

Starting from a homogeneous amorphous state of $Ge_2Sb_2Te_5$ the metastable $Ge_2Sb_2Te_5$ structure requires much less dedicated diffusion and ordering than the stable one and the crystallization rate (i.e., growth rate) can thus be higher. In Refs. 5 and 6 it is in principle shown that the growth rate of the metastable crystalline phase depends on the "embryos." The crystallization proceeds in 10 ns in case of Ref. 6 where embryos are already present, whereas the crystallization time increases to 100 ns if embryos are absent. This suggests that arguments based on the amorphous/crystalline interfacial energy γ are more important than arguments based on diffusion and ordering. The interfacial energy together with the strain energy involved determines the critical size r^* of a stable crystalline nucleus in the amorphous matrix and the activation energy ΔG^* to arrive at this size.[22] For a spherical nucleus it holds:[22]

$$r^* = \frac{2\gamma}{(\Delta G_V - \Delta G_S)},$$

$$\Delta G^* = \frac{16\pi\gamma^3}{3(\Delta G_V - \Delta G_S)^2},$$

where ΔG_S is the strain energy in the nucleus and surrounding matrix introduced per unit volume of the nucleus, and ΔG_V is the difference in Gibbs-free energy per unit of volume of bulk between the phase in the matrix and the one that develops in the nucleus. The last term is the driving force, while the other term opposes the transformation. It is fairly safe to state that both the interfacial energy and the strain energy corresponding to a nucleus with the NaCl-type structure is clearly lower than for the rhombohedral structure with its larger c'-axis. The NaCl structure more closely resembles the surrounding amorphous state. Therefore, although the driving force (ΔG_V) for crystallization in the metastable structure is definitely lower, this is easily outweighed by the

lower interfacial and strain energy. Note that in the activation energy the interfacial energy γ goes to the power of 3 whereas the driving force ΔG_V goes to the power of 2. Since it is now well-proven that in phase change optical recording Ge–Sb–Te shows growth-limited (i.e., nucleation-driven) crystallization as opposed to for instance, Ag–In–Sb–Te that shows nucleation-limited crystallization,[9] it is particularly clear that nuclei form very easily in Ge–Sb–Te. This is fully consistent with the physical picture presented here based on the difference in stable and metastable crystal structures.

VI. CONCLUSIONS

The crystal structures of $Ge_xSb_2Te_{3+x}$ $(x=1,2,3)$ phase change material have been determined based on electron diffraction and HRTEM. $Ge_2Sb_2Te_5$ can be described as having a trigonal structure with a primitive hexagonal unit cell (e.g., space group $P\text{-}3m1$) with $a'=0.425$ nm and $c'=1.827$ nm, and with a stacking sequence of pure Te–Ge–Te–Sb–Te–Te–Sb–Te–Ge– basal planes along the c'-axis of the unit cell. This basic repeat unit contains one Ge–Te double layer less in $GeSb_2Te_4$ and one more in $Ge_3Sb_2Te_6$. Because the unit cell requires a c'-axis with $3n$ basal planes, both $GeSb_2Te_4$ and $Ge_3Sb_2Te_6$ contain three such basic repeat units per unit cell. Thus, the lattice parameters of $GeSb_2Te_4$ and $Ge_3Sb_2Te_6$ are $a'=0.425$, $c'=4.10$ nm and $a'=0.425$, $c'=6.26$ nm, respectively, and in both cases the space group is $R\text{-}3m$. The stacking sequence proposed here for $GeSb_2Te_4$ and $Ge_2Sb_2Te_5$ differs from the ones proposed earlier and no previous report on $Ge_3Sb_2Te_6$ apparently exists.

The $Ge_xSb_2Te_{3+x}$ crystals were grown from molten $Ge_2Sb_2Te_5$, and higher cooling rates probably imply a larger fraction of $GeSb_2Te_4$ and $Ge_3Sb_2Te_6$ crystals and certainly imply a larger amount of stacking disorder of close-packed planes in the crystals. Basic units in all the crystals, also with larger fraction of disorder, are a Ge–Te double layer also present in binary GeTe and a Te–Sb–Te–Te–Sb– repeat unit and a Sb–Te double layer both also present in binary Sb_2Te_3. It may be that all possible stable crystal structures in the ternary Ge–Sb–Te system will be built out of these basic units and will have a,b,c stacking of the close-packed planes.

The fast crystallization rate from solid amorphous $Ge_2Sb_2Te_5$ to the metastable NaCl-type crystal structure can be understood, because the interfacial and strain energy associated with a nucleus with the metastable NaCl-type crystal structure is lower than with the complex stable trigonal structure (i.e., nucleation argument) and also because the former structure requires much less dedicated diffusion and ordering (i.e., growth argument).

[1] H. J. Borg and R. van Woudenberg, J. Magn. Magn. Mater. **193**, 519 (1999).
[2] T. H. Jeong, M. R. Kim, H. Seo, S. J. Kim, and S. Y. Kim, J. Appl. Phys. **86**, 774 (1999).
[3] I. Friedrich, V. Weidenhof, W. Njoroge, P. Franz, and M. Wuttig, J. Appl. Phys. **87**, 4130 (2000).
[4] V. Weidenhof, N. Pirich, I. Friedrich, S. Ziegler, and M. Wuttig, J. Appl. Phys. **88**, 657 (2000).
[5] P. K. Khulbe, E. M. Wright, and M. Mansuripur, J. Appl. Phys. **88**, 3926 (2000).
[6] V. Weidenhof, I. Friedrich, S. Ziegler, and M. Wuttig, J. Appl. Phys. **89**, 3168 (2001).
[7] T. Nonaka, G. Ohbayashi, Y. Toriumi, Y. Mori, and H. Hashimoto, Thin Solid Films **370**, 258 (2000).
[8] N. Yamada and T. Matsunaga, J. Appl. Phys. **88**, 7020 (2000).
[9] G.-F. Zhou, Mater. Sci. Eng., A **304–306**, 73 (2001).
[10] N. Yamada, E. Ohno, N. Akahira, N. Nishiuchi, K. Nagata, and M. Takao, Jpn. J. Appl. Phys. **26**, 61 (1987).
[11] V. Weidenhof, I. Friedrich, S. Ziegler, and M. Wuttig, J. Appl. Phys. **86**, 5879 (1999).
[12] I. I. Petrov, R. M. Imamov, and Z. G. Pinsker, Sov. Phys. Crystallogr. **13**, 339 (1968).
[13] *ASM Handbook, Alloy Phase Diagrams*, edited by H. Baker (ASM International, Materials Park, Ohio, 1992), Vol. 3.
[14] *Structure Reports*, edited by W. P. Pearson (International Union of Crystallography, New York, 1953), Vol. 17, p. 44.
[15] J. Goldak, C. S. Barrett, D. Innes, and W. Youdelis, J. Chem. Phys. **44**, 3323 (1966).
[16] R. W. G. Wyckoff, *Crystal Structures*, 2nd ed. (Interscience, New York, 1963), Vol. 2, pp. 29–31.
[17] K. A. Agaev and A. G. Talybov, Sov. Phys. Crystallogr. **11**, 400 (1966).
[18] R. Kilaas, distributed by Total Resolution, 20 Florida Ave., Berkeley, CA 94707.
[19] D. Van Dyck and M. Op de Beeck, Ultramicroscopy **64**, 99 (1996).
[20] M. Op de Beeck and D. Van Dyck, Ultramicroscopy **64**, 153 (1996).
[21] P. G. Self, R. W. Glaisher, and A. E. C. Spargo, Ultramicroscopy **18**, 49 (1985).
[22] D. A. Porter and K. E. Easterling, *Phase Transformations in Metals and Alloys* (Van Nostrand Reinhold, New York, 1981), pp. 265–271.